

## Temperature Dependence of the Effective Masses in PbTe†

HENRY A. LYDEN\*

*Massachusetts Institute of Technology, Cambridge, Massachusetts*

(Received 11 February 1964)

The study presented here includes experimental data obtained from three *n*-type and two *p*-type single-crystalline samples of PbTe. Measurements of the Hall coefficient, thermoelectric power, and electrical conductivity have been made between 77 and 300°K, and infrared reflectivity data have been obtained at 4, 77, 190, and 300°K. The free-carrier concentration of all samples is in the range  $2\text{--}4 \times 10^{18}$  carriers/cm<sup>3</sup>. From the thermoelectric power, we have deduced the temperature dependence of the reduced Fermi potential for each sample and have calculated the density-of-states effective mass  $m_d$ . A pronounced temperature dependence has been observed for  $m_d$ . At 77°K we have observed that  $m_{dn}=0.20 m_o$  and  $m_{dp}=0.14 m_o$ , whereas at 300°K they have increased monotonically to the values  $m_{dn}=0.30 m_o$  and  $m_{dp}=0.25 m_o$ . The minimum of the infrared reflectivity has been utilized in obtaining values for the conductivity effective mass  $m_c$ . The temperature dependence noted for  $m_c$  has been very similar to that obtained for  $m_d$ . At 4°K we obtained the values  $m_{cn}=0.050 m_o$  and  $m_{cp}=0.039 m_o$ , and they increase monotonically to their values at 300°K which have been determined to be  $m_{cn}=0.103 m_o$  and  $m_{cp}=0.11 m_o$ . These values of the effective masses have been used to deduce the number of equivalent ellipsoids of constant energy  $N_v$ . For the conduction band, we find  $N_v=4$  indicating that the (111) minima are at the edge of the zone. For the valence band we are unable to be as quantitative because of the presence of a maximum at the center of the zone as well as the maxima positioned along the  $\langle 111 \rangle$  axes. However, assuming that all ellipsoids are equivalent, we calculate  $N_v \approx 2.5$  from which it is inferred that the zone-centered maximum plays a prominent role in the energy-band picture.

### INTRODUCTION

THE energy-band structure gives rise to the effective masses of free carriers in solids. These effective masses in turn directly affect the free-carrier mobility within the solid. When it is possible to describe a scattering process in terms of a relaxation time  $\tau$ , the free-carrier mobility takes the form

$$\mu = (e/m_c)\langle\tau\rangle, \quad (1)$$

where  $e$  is the electronic charge,  $m_c$  is the conductivity effective mass, and  $\langle\tau\rangle$  is the relaxation time averaged over the kinetic energy of all of the free electrons. Equation (1) can be considered to define  $m_c$ . Another effective mass, the density-of-states effective mass  $m_d$ , arises when, for the purpose of statistical computation, the distribution of allowed energy levels in the conduction (valence) band is replaced by a single level having a degeneracy  $N_n(N_p)$  at the band edge. This effective density-of-states is given by the relation<sup>1</sup>

$$N_n = 2 \left[ \frac{2\pi m_{dn} k T}{h^2} \right]^{3/2}. \quad (2)$$

$N_p$  is given by the same relation with the substitution of

\* Present address: Energy Conversion, Inc., Cambridge, Massachusetts.

† This paper is based upon a dissertation by the author submitted in partial fulfillment of the degree of Doctor of Science to the Electrical Engineering Department of the Massachusetts Institute of Technology and published as Scientific Report No. 7 under Contract No. AF 19(604)-4153 (January 1962). Air Force Cambridge Research Laboratory document number AFCRL-62-129 (unpublished).

<sup>1</sup> W. Shockley, *Electrons and Holes in Semiconductors* (D. Van Nostrand Company, Inc., Princeton, New Jersey, 1950), Chaps. 10 and 11.

$m_{dp}$  for  $m_{dn}$ . In Eq. (2),  $k$  is Boltzmann's constant,  $T$  is the absolute temperature, and  $h$  is Planck's constant.

For the case of acoustical-mode lattice scattering, the deformation-potential theory yields a mobility of the form<sup>1</sup>:

$$\mu \propto m_c^{-1} m_d^{-3/2} T^{-1} \langle E^{-1/2} \rangle, \quad (3)$$

where  $E$  is the thermal kinetic energy of the free carriers. In the nondegenerate case, the average thermal energy is proportional to the temperature, and the mobility has an apparent temperature dependence of  $T^{-3/2}$ . However, an additional temperature dependence can enter through the effective masses.

In passing, we note that while  $m_c = m_d$  for spherical surfaces of constant energy, they take on a more complex form when the surfaces are not spheres at the center of the Brillouin zone but are ellipsoids-of-revolution along a set of symmetry axes of the zone. In the case of cubic symmetry as in PbTe, it is found that:

$$m_d = (m_l m_t^2)^{1/3} \quad (4)$$

and

$$\frac{1}{m_c} = \frac{1}{3} \left( \frac{1}{m_l} + \frac{2}{m_t} \right), \quad (5)$$

where  $m_l$  is the value of the effective-mass tensor associated with the longitudinal axis of the ellipsoidal energy surface and  $m_t$  is that associated with each of the two transverse axes of the surface.

From Eq. (3), one sees that the effective masses play an important role in the standard mobility theory. Also, it is seen that both the conductivity and the density-of-states effective masses are involved. It is the purpose of this paper to establish the magnitude and temperature variation of both  $m_d$  and  $m_c$  for *n*- and *p*-type PbTe.

## PROCEDURE

Three *n*-type and two *p*-type single crystals were prepared. On these single crystalline samples we have conducted the following measurements and analysis:

(i) The thermoelectric power  $Q$  of these samples was measured over the temperature range 77–300°K. In order to relate these results to the theoretical expressions a fundamental assumption has been made to the effect that the predominant scattering mechanism is acoustical-mode lattice scattering. (There is considerable experimental evidence which indicates that such an assumption is justified. This evidence is reviewed at a later point in this paper.) On the basis of this assumption, the data obtained for  $Q$  have been used to calculate the reduced Fermi potential  $\eta = E_f/kT$  as a function of temperature for each sample. (Here  $E_f$  is the Fermi energy relative to the band edge.)

(ii) Hall measurements at liquid-nitrogen temperatures were used to determine the free-carrier concentration  $N$  in each of the five samples. Knowing this and  $\eta$ , the density-of-states effective mass  $m_d$  has been calculated over the temperature range 77–300°K.

(iii) The electrical conductivity was measured throughout this same temperature range. With the values of  $N$  obtained above, this has been used to calculate the mobility of free carriers  $\mu$  for these temperatures.

(iv) The infrared reflectivity of these same samples was measured at 4, 77, 190, and 300°K. These data, along with the data for  $N$  and  $\mu$ , have been used to calculate the conductivity effective mass  $m_c$  as a function of temperature following the procedure developed by the author.<sup>2</sup>

The thermoelectric power is analyzed by means of the theoretical expression which is applicable for Fermi-Dirac statistics, ellipsoidal energy surfaces, and extrinsic conduction, namely<sup>3</sup>:

$$Q = \pm \left[ \frac{k \left[ (s + \frac{5}{2}) F_{s+3/2} \right]}{e \left[ (s + \frac{3}{2}) F_{s+1/2} \right]} - \eta \right], \quad (6)$$

where  $s$  is characteristic of the scattering mechanism and is the exponent of the free-carrier kinetic energy in the relaxation time  $\tau = \tau_0 E^s$ , and  $F_\phi$  is a Fermi-Dirac integral of the form

$$F_\phi(\eta) = \int_0^\infty \xi^\phi f_0(\xi, \eta) d\xi \quad (7)$$

in which  $\xi$  is the reduced kinetic energy of the free carriers  $E/kT$ , and  $f_0$  is the Fermi distribution function

$$f_0(\xi, \eta) = 1 / (1 + e^{(\xi - \eta)}). \quad (8)$$

<sup>2</sup> H. Lyden, Phys. Rev. **134**, A1106 (1964).

<sup>3</sup> H. Goldsmid, *Applications of Thermoelectricity* (Methuen and Company Ltd., London, 1960), p. 33.

The value to be assigned to the parameter  $s$  in Eq. (6) is of course dependent upon the scattering mechanism which is dominant in the scattering of free carriers in PbTe. The temperature dependence of the free-carrier mobility is such that there is some question as to what this dominant scattering mechanism is. However, there is experimental evidence which serves as a basis for assuming that acoustical-mode lattice scattering predominates above 100–150°K. If such is the case, the value to be assigned is  $s = -\frac{1}{2}$ .

Probably the most direct method for evaluating the energy dependence of the relaxation time is through the determination of the Nernst-Ettingshausen effect. A very detailed investigation of this effect in PbS, PbSe, and PbTe has been reported in the literature.<sup>4</sup> In all, the Nernst-Ettingshausen effect was measured in seven samples, three of which were PbTe. In every case the results indicated a value of  $s$  somewhere in the range  $-\frac{1}{2} < s < 0$ . Since the choices considered were scattering by: the acoustical modes of a covalent lattice for which  $s = -\frac{1}{2}$ , the vibrational modes of an ionic lattice above the Debye temperature ( $\Theta \approx 130^\circ\text{K}$  for PbTe)<sup>5</sup> for which  $s = +\frac{1}{2}$ , or ionized impurities for which  $s = +\frac{3}{2}$ , the conclusion reached in the above analysis was that lattice bonding must be predominately covalent (as opposed to ionic) and that the scattering is dominated by the acoustical modes of the lattice.

Moreover, this same conclusion was reached in an analysis in which the Lorentz number, in the Wiedemann-Franz law for the thermal conductivity of free carriers, was determined for PbSe<sup>6</sup> and for PbTe.<sup>7</sup> The same result has also been inferred from studies of the thermoelectric power of PbTe.<sup>8</sup>

Probably the most significant feature of the investigations into the scattering mechanism is that none have supported any other hypothesis except that  $s \approx -\frac{1}{2}$ . Consequently, this is the value of  $s$  that is used in the subsequent evaluation of the thermoelectric power data.

The Hall effect data are analyzed by means of the theoretical equation which has been derived for the Hall coefficient in crystals having cubic symmetry and ellipsoidal surfaces of constant energy along the symmetry axes. This equation for the Hall coefficient is<sup>9</sup>:

$$R = \frac{b}{Ne} \left[ \frac{3K(K+2)}{(2K+1)^2} \right], \quad (9)$$

where  $b$  is a numerical factor which, for the assumed

<sup>4</sup> I. Tsidi'kovskii, Phys. Metals Metallog. **8**, 16 (1959).

<sup>5</sup> D. Parkinson and J. Quarrington, Proc. Phys. Soc. (London) **A67**, 569 (1954).

<sup>6</sup> E. Devyat'kova and I. Smirnov, Fiz. Tverd. Tela **2**, 1984 (1960) [English transl.: Soviet Phys.—Solid State **2**, 1786 (1961)].

<sup>7</sup> E. Devyat'kova and I. Smirnov, Fiz. Tverd. Tela **3**, 2310 (1961) [English transl.: Soviet Phys.—Solid State **3**, 1675 (1962)].

<sup>8</sup> E. Gershtein, T. Savitskaia, and L. Stilbans, Zh. Techn. Fiz. **27**, 2472 (1957) [English transl.: Soviet Phys.—Tech. Phys. **2**, 2302 (1957)].

<sup>9</sup> R. Allgaier and W. Scanlon, Phys. Rev. **111**, 1029 (1958).

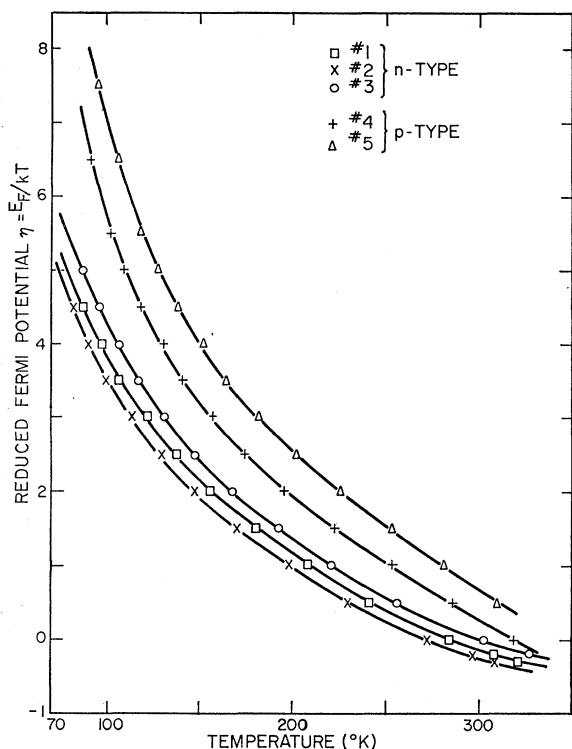


FIG. 1. The reduced Fermi potential as a function of temperature determined from the thermoelectric power assuming acoustical-mode scattering.

acoustical scattering, varies between the limits  $3\pi/8$  and 1 corresponding to classical and degenerate statistics respectively, and  $K$  is the effective mass ratio  $m_l/m_t$  (assuming that the relaxation time is isotropic). The value of the bracketed term in Eq. (9) is determined using values of  $K$  which are reported in the literature as a result of magnetoresistivity studies.<sup>10,11</sup> These values reported for  $K$  are not in exact agreement with each other. However, they do indicate that  $K$  probably lies in the range  $3 < K < 6$  for all temperatures below 300°K. Over this range of  $K$  values, the bracketed term is not a strongly varying function. Its corresponding range of values is between 0.92 and 0.85. For this reason, the bracketed term is assigned the value of 0.9 in the subsequent analysis of the Hall data for both  $n$ -type and  $p$ -type material.

TABLE I. Values determined for the relative dielectric constant of the lattice in the absence of any contribution from free carriers using Eq. (11).

| $T$ (°K) | $\epsilon_\infty = n_\infty^2$ |
|----------|--------------------------------|
| 7        | 40.3                           |
| 77       | 37.5                           |
| 190      | 34.3                           |
| 300      | 31.8                           |

<sup>10</sup> R. Allgaier, Phys. Rev **119**, 554 (1960)

<sup>11</sup> K. Cuff, M. Ellett, and C. Kuglin, J. Appl. Phys. Suppl. **32**, 2179 (1961).

The conductivity effective mass is obtained from the frequency of the free-carrier reflectivity minimum in the far infrared using the following equation<sup>2</sup>:

$$m_c^{*3} \frac{(3\epsilon_\infty - 1)(1/\Omega^2) + 5 + 8\Omega^2}{4\epsilon_\infty(\epsilon_\infty - 1)(1 + 3\Omega^2)} C m_c^{*2} + \frac{(3\epsilon_\infty - 2)(1 + 2\Omega^2)}{2\epsilon_\infty(\epsilon_\infty - 1)^2(1 + 3\Omega^2)} C^2 m_c^{*} + \frac{C^3}{4\epsilon_\infty(\epsilon_\infty - 1)^2(1 + 3\Omega^2)} = 0, \quad (10)$$

where  $m_c^* = m_c/m_0$  and  $m_0$  is the free-electron mass,  $\Omega = \omega_0\langle\tau\rangle$ ,  $C = Ne^2/m_0\epsilon_0\omega_0^2$ ,  $\omega_0$  is the angular frequency corresponding to the reflectivity minimum,  $\epsilon_0$  is the dielectric constant of free space, and  $\epsilon_\infty$  is the relative dielectric constant of the medium in the absence of any contribution from free carriers at very high frequencies. [The discussion of the justification for using Eq. (10) in the determination of the conductivity effective mass is deferred to a later section of this paper.]

Of the parameters involved in the evaluation of Eq. (10), only  $\epsilon_\infty$  has not been determined in this investigation. Values for this parameter can be found in the literature. For example, along with his data for the absorption edge corresponding to the energy-gap transitions in the PbS group of compounds, Avery<sup>12</sup> presents values for the refractive index at  $6\mu$  for  $T = 300^\circ\text{K}$ . For PbTe he gives the value  $n_\infty = 5.48 \pm 0.10$ . Moss<sup>13</sup> first suggested a value  $n_\infty = 5.5$  but has recently experimentally determined the value  $n_\infty = 5.64 \pm 0.03$ .<sup>14</sup> This last value represents the most accurate determination of this parameter to date, and it has been selected for subsequent calculations. Since  $\epsilon_\infty = n_\infty^2$ , this yields the value  $\epsilon_\infty = 31.8$  at  $T = 300^\circ\text{K}$ . Moreover, Moss has also suggested that for PbTe the relation between  $n_\infty$  and the wavelength of the absorption edge  $\lambda_g$  obeys the equation<sup>13</sup>

$$n_\infty^4/\lambda_g = \epsilon_\infty^2/\lambda_g = \text{constant}, \quad (11)$$

where the constant is not the same as that observed for most photoconductors ( $\approx 77$ ), but the relationship apparently holds nevertheless.<sup>14a</sup> Now, the energy gap in PbTe, including its temperature dependence, has been studied by Gibson,<sup>15</sup> Avery,<sup>12</sup> and Scanlon<sup>16</sup> and their results are in close agreement below  $\approx 400^\circ\text{K}$ . They show that  $E_g \approx 0.20$  eV at  $0^\circ\text{K}$  and that it increases at a rate of  $4 \times 10^{-4}$  eV deg<sup>-1</sup>. Thus, combining

<sup>12</sup> D. Avery, Proc. Phys. Soc. (London) **B67**, 2 (1954).

<sup>13</sup> T. Moss, Proc. Phys. Soc. (London) **B66**, 141 (1953).

<sup>14</sup> A. Walton and T. Moss, Proc. Phys. Soc. (London) **81**, 509 (1963).

<sup>14a</sup> Note added in proof. The author wishes to acknowledge the point that the temperature dependence of  $n_\infty$  could have been determined by extending the reflectivity measurements to shorter wavelengths. Unfortunately, the equipment could not be modified to make measurements at these wavelengths.

<sup>15</sup> A. Gibson, Proc. Phys. Soc. (London) **B65**, 378 (1952).

<sup>16</sup> W. Scanlon, Phys. Chem. Solids **8**, 423 (1959).

TABLE II. Results from the analysis of the Hall data using Eq. (9).

| Sample no. | Type     | Free carriers/cm <sup>3</sup> |
|------------|----------|-------------------------------|
| 1          | <i>n</i> | 2.9 × 10 <sup>18</sup>        |
| 2          | <i>n</i> | 2.2 × 10 <sup>18</sup>        |
| 3          | <i>n</i> | 3.8 × 10 <sup>18</sup>        |
| 4          | <i>p</i> | 3.3 × 10 <sup>18</sup>        |
| 5          | <i>p</i> | 3.6 × 10 <sup>18</sup>        |

the data of the thermal behavior of the energy gap with the value  $n_{\infty} = 5.64$  at 300°K, it is possible to calculate  $n_{\infty}$  and  $\epsilon_{\infty}$  for other temperatures below 400°K using Eq. (11). The values calculated are shown in Table I.

### EXPERIMENTAL RESULTS AND ANALYSIS

The first measurement to be considered is the thermoelectric power. Making the assumption that  $s = -\frac{1}{2}$ , Eq. (6) becomes

$$Q = \pm (k/e) [(2F_1/F_0) - \eta]. \quad (12)$$

This equation has been evaluated for  $\eta$  with the aid of a table of Fermi-Dirac functions.<sup>17</sup> The results of these calculations are presented in Fig. 1.

We found  $\eta > 4$  at 77°K in all samples indicating that they can be considered to be completely degenerate at that temperature. This has significance with respect to the Hall data. Referring to Eq. (9) one can be assured that the numerical factor  $b$  is unity for all samples at 77°K. On the basis of this result,  $b = 1$  at 77°K, and using the approximation that the bracketed term of Eq. (9) is given the value 0.9, the Hall data have been utilized to determine the free-carrier concentration of the five samples. The results are presented in Table II.

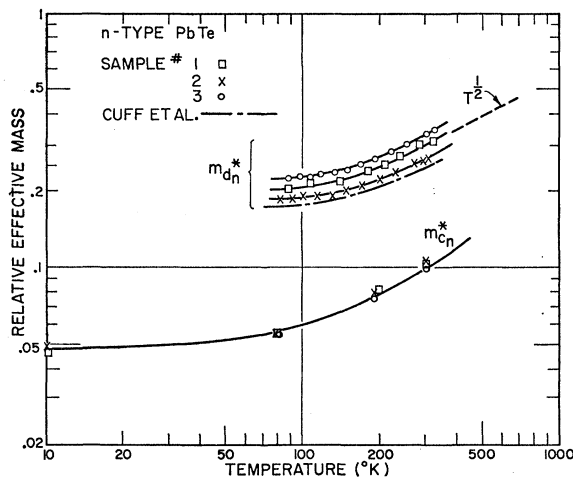


FIG. 2. The relative effective masses  $m_d^*$  and  $m_c^*$  for *n*-type PbTe as a function of temperature. The results for  $m_d^*$  of Cuff *et al.* of Ref. 19 are shown for comparison.

<sup>17</sup> See Ref. 3, p. 116.

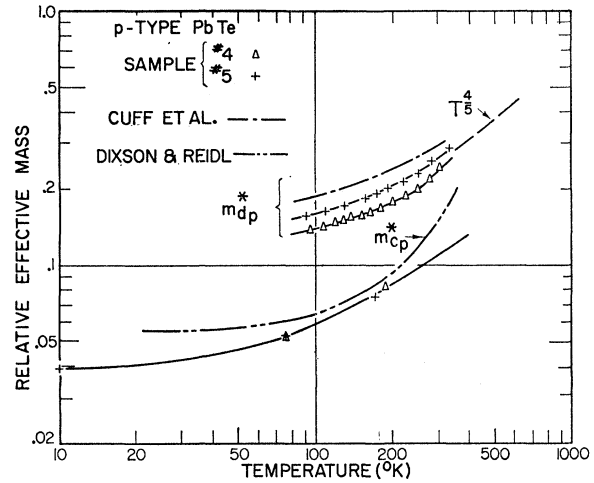


FIG. 3. The relative effective masses  $m_d^*$  and  $m_c^*$  for *p*-type PbTe as a function of temperature. The results for  $m_d^*$  of Cuff *et al.* of Ref. 19 are shown for comparison as well as the results for  $m_c^*$  of Dixon and Reidl of Ref. 24.

Having established the free-carrier concentration and the temperature dependence of  $\eta$ , it is possible to calculate a value for the density-of-states effective mass. This can be obtained from the relation

$$m_d^* = \frac{m_d}{m_0} = \left( \frac{N}{4\pi} \right)^{2/3} \left( \frac{h^2}{2m_0kT} \right) [F_{1/2}(\eta)]^{-2/3}. \quad (13)$$

The results of this calculation are presented in Figs. 2 and 3. The data show that  $m_d^*$  has a very definite temperature dependence. This is in qualitative agreement with findings in<sup>18</sup> PbSe and in<sup>19</sup> PbTe but contrary to those of another report for PbTe.<sup>20</sup> At temperatures near 100°K, the apparent temperature dependence is very slight. However, at 300°K for *n*-type material  $m_{dn}^* \propto T^{0.5}$ , and for *p*-type this dependence is slightly greater,  $m_{dp}^* \propto T^{0.8}$ . The values for  $m_d$  presented here can be seen to agree with those of Cuff *et al.*<sup>19</sup> in both their absolute magnitudes and temperature dependences.

The free-carrier mobility has been determined between 77 and 300°K. For this determination, the electrical conductivity was measured over the above temperature range. Noting that, for an extrinsic conductor, this parameter may be represented by the formula

$$\sigma = Ne\mu, \quad (14)$$

it follows directly from Eqs. (14) and (9) that the

<sup>18</sup> I. Smirnov, B. Moizhes, and E. Nensberg, *Fiz. Tverd. Tela* **2**, 1992 (1960) [English transl.: *Soviet Phys.—Solid State* **2**, 1793 (1961)].

<sup>19</sup> K. Cuff, M. Ellett, and C. Kuglin, *Proceedings of the International Conference on the Physics of Semiconductors, Exeter 1962* (The Institute of Physics and the Physical Society, London, 1962), pp. 316–22.

<sup>20</sup> E. Miller, K. Komarek, and I. Cadoff, *J. Appl. Phys.* **32**, 2457 (1961).

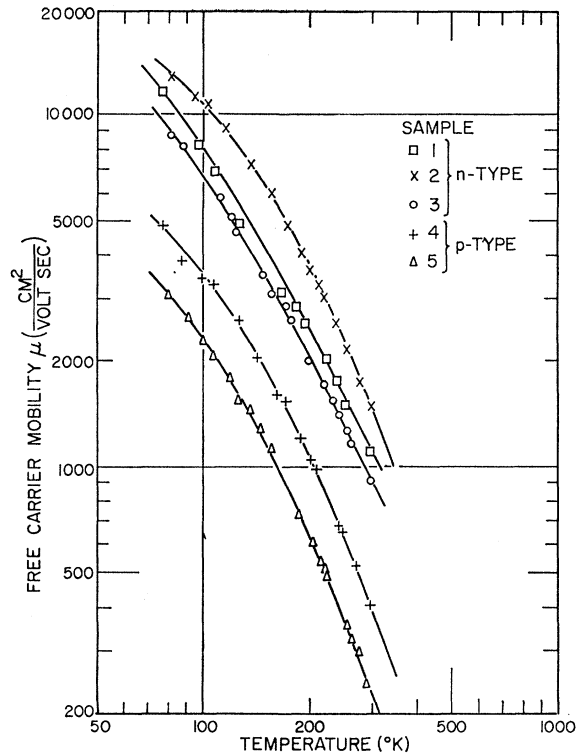


FIG. 4. The free-carrier mobility of 3 *n*- and 2 *p*-type samples of PbTe as a function of temperature.

mobility may be calculated from the relation

$$\mu = R_{77} \sigma \left[ \frac{(2K+1)^2}{3K(K+2)} \right]. \quad (15)$$

The mobility values determined using Eq. (15) are shown in Fig. 4.

This brings us to the point where we are in a position to present and analyze the infrared reflectivity measurements which have been made in the region of the free-carrier reflectivity minimum. The infrared reflectivity of one of the *n*-type samples is presented in Fig. 5. The qualitative features that are readily apparent are the following:

- (i) The reflectivity does exhibit a minimum in this range of wavelengths which, however, becomes broader and more shallow as the temperature increases.
- (ii) The position of the minimum has a distinct temperature dependence, moving to longer wavelengths as the temperature is increased.

To determine the conductivity effective mass from the reflectivity, we have utilized Eq. (10). For this calculation the angular frequency of minimum reflectivity, the free-carrier concentration, the value and temperature dependence of the free-carrier mobility and of the dielectric constant of the lattice at very high frequencies are required. The temperature dependence

TABLE III. Data pertinent to the calculation of the conductivity effective masses of 3 *n*- and 2 *p*-type samples of PbTe.

| Sample no. | <i>T</i> (°K) | $\mu$ (m <sup>2</sup> /V-sec) | $\lambda_0$ (μ) | $m_c^*$ |
|------------|---------------|-------------------------------|-----------------|---------|
| 1          | 4             | undetermined                  | 26.4            | 0.046   |
|            | 77            | 1.15                          | 28.2            | 0.056   |
|            | 194           | 0.26                          | 31.2            | 0.084   |
|            | 300           | 0.12                          | 32.5            | 0.103   |
| 2          | 4             | undetermined                  | 31.4            | 0.049   |
|            | 77            | 1.4                           | 32.5            | 0.056   |
|            | 185           | 0.43                          | 35.9            | 0.081   |
|            | 300           | 0.14                          | 37.8            | 0.108   |
| 3          | 77            | 0.97                          | 24.5            | 0.056   |
|            | 188           | 0.23                          | 26.2            | 0.075   |
|            | 300           | 0.095                         | 27.3            | 0.098   |
| 4          | 77            | 0.48                          | 24.6            | 0.053   |
|            | 170           | 0.15                          | 27.1            | 0.076   |
| 5          | 4             | undetermined                  | 21.7            | 0.039   |
|            | 77            | 0.32                          | 23.3            | 0.053   |
|            | 187           | 0.072                         | 25.6            | 0.083   |

of the last parameter  $\epsilon_\infty$  has been calculated from Eq. (11) with the results listed in Table I. Other pertinent information is presented in Table III along with the calculated values for the conductivity effective mass. The data for  $m_c^*$  are also shown plotted as a function of temperature in Figs. 2 and 3. It should be noted in conjunction with Table III that the value of the mobility is not required to calculate  $m_c^*$  at 4°K, since at this temperature the approximation  $\Omega^2 \gg 1$  is valid. Consequently, the parameter  $\Omega$  cancels out of Eq. (10) (except in the last term which is negligibly small).<sup>21</sup>

It is apparent from Figs. 2 and 3 that the conductivity effective mass calculated in this way exhibits a temperature dependence, increasing with increasing temperature. The actual rate of increase is very similar to that which is observed in the density-of-states effective mass. This result is consistent with the fact that the

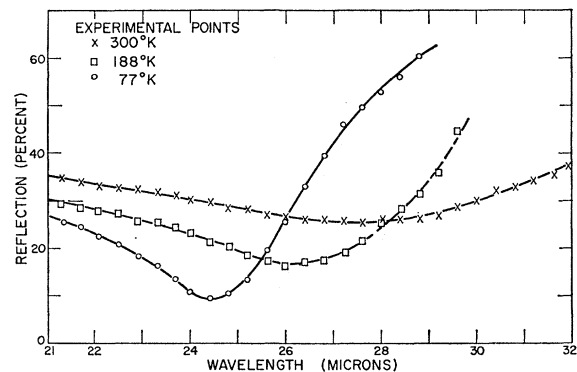


FIG. 5. The percent reflection of *n*-type sample No. 3 measured at 77, 188, and 300°K as a function of wavelength in the region of the reflectivity minimum.

<sup>21</sup> The slight difference between the values for  $m_c^*$  presented here and those originally presented in Air Force Cambridge Research Document No. AFCRL-62-129 arises from the utilization of the more recently reported value for  $n_\infty$  (= 5.64) instead of the value (5.48) presented in Ref. 12.

anisotropy ratio  $K$  does not change significantly with temperature, say from  $5.5_{-1.5}^{+2.5}$  at  $4^\circ\text{K}$  to  $4.0 \pm 0.5$  at  $300^\circ\text{K}$  for  $n$ -type<sup>11</sup> PbTe and from 4.2 at  $77^\circ\text{K}$  to 4.7 at  $300^\circ\text{K}$  for  $p$ -type.<sup>10</sup> The consistency of these results follows from the relationships between these quantities, namely

$$m_d^* = m_i^* N_v^{2/3} K^{1/3}, \quad (16)$$

where  $N_v$  is the number of equivalent ellipsoids of constant energy in the conduction or valence band, and

$$m_c^* = m_i^* 3K / (2K + 1). \quad (17)$$

For the  $K$  values noted, the factors involving  $K$  in Eqs. (16) and (17) are limited to the range of values

$$1.59 < K_n^{1/3} < 1.76, \quad 1.61 < K_p^{1/3} < 1.67$$

and

$$1.33 < 3K_n / (2K_n + 1) < 1.37,$$

$$1.34 < 3K_p / (2K_p + 1) < 1.36.$$

From which it follows that the factor contributing most significantly to the temperature dependence of both  $m_d^*$  and  $m_c^*$  is  $m_i^*$ , thereby producing a similar temperature variation in each case. The fact that a similar temperature dependence was observed in both  $m_d^*$  and  $m_c^*$  increases one's confidence in the validity of the results, since these two were determined by very different methods.

Moreover, from Eqs. (16) and (17) and from the data for the effective masses, it is possible to determine the number of equivalent ellipsoids in the conduction and valence bands:

$$N_v^{2/3} = (m_d^* / m_c^*) [3K^{2/3} / (2K + 1)]. \quad (18)$$

The results for the conduction band are listed in Table IV. The results indicate that a four-valley model for the conduction band is to be preferred over an eight-valley model. This result coincides with that obtained by Cuff *et al.*<sup>11</sup> at  $4^\circ\text{K}$ . Moreover, the fact that these effective masses result in values of  $N_v$  so close to a theoretical value of 4, a value which has already been deduced at  $4^\circ\text{K}$ , further increases our confidence in the temperature dependences and in the absolute values of these masses.

Another comparison between the results of this investigation and of others is afforded at  $4^\circ\text{K}$  where a value for  $m_i$  in the conduction band has been determined from the ratio of the oscillatory magnetoresis-

tance obtained at  $1.7^\circ$  and at  $4^\circ\text{K}$  for a given magnetic field.<sup>11</sup> The value reported is  $m_i = 0.030 \pm 0.005$ . Using the value of  $K$  given in the same report,  $K = 5.5_{-1.5}^{+2.5}$ , a conductivity effective mass can be calculated. This calculation yields  $m_c^* = 0.041 \pm 0.008$  as compared with  $m_c^* = 0.048 \pm 0.005$  which has been obtained in this investigation. The agreement is good, especially in view of the fact that the samples investigated here have a carrier concentration which is an order-of-magnitude greater than for the samples utilized in Ref. 11, and any non-parabolicity in the conduction band tends to produce higher effective masses in the material of higher degeneracy.<sup>19</sup>

It has been noted that the data are compatible with a four-valley model for the conduction band. However, a more complicated model, such as a minimum at the center of the zone in addition to the four minima at the boundary as has been recently proposed,<sup>11</sup> cannot definitely be ruled out. Moreover, in the above analysis it was necessary to utilize  $K$  values reported in the literature. If we now invert the procedure used above, by assuming that the number of ellipsoids is four, it is possible to obtain values of  $K$  and then to compare these values with those reported in the literature. The results of this computation are listed in Table V. The values of  $K$  that are obtained using this inverted procedure are slightly different from those used in the initial computation of  $N_v$  but they are nevertheless comparable to those reported in Ref. 11.

It should be noted that  $K$  is actually more than a ratio of  $m_l/m_t$ . The complete expression is  $K = m_l/\tau_l/m_t\tau_t$ , where  $\tau_l$  and  $\tau_t$  are the longitudinal and transverse relaxation times. A change in  $K$  with temperature can be indicative of a change in the anisotropy of the  $\tau$ 's which in turn can be indicative of a changing scattering mechanism. On the other hand, if  $\tau$  is assumed to be isotropic, then  $K$  can be considered as simply the ratio  $m_l/m_t$ . The values for  $m_i^*$  and  $m_t^*$  listed in Table V have been calculated on this basis, i.e., an isotropic relaxation time. It is interesting to note that  $m_i^*$  changes by almost 100% with respect to its value at  $77^\circ\text{K}$  while  $m_t^*$  remains relatively constant at 0.3 throughout the temperature range. Thus, if the assumption of an isotropic relaxation time is valid, this result implies that the ellipsoids of constant energy becomes less prolate with increasing temperature.

In considering the results for  $p$ -type material, the presence of a valence-band maximum at the zone center, in addition to the ones along the  $\langle 111 \rangle$  axes, greatly

TABLE IV. Data used in Eq. (18) for the determination of the number of equivalent ellipsoids in the conduction band.

| $T(^{\circ}\text{K})$ | $m_d^*$<br>(av) | $m_c^*$ | $K$<br>(Ref. 11) | $N_v$ |
|-----------------------|-----------------|---------|------------------|-------|
| 77                    | 0.20            | 0.056   | 5.5              | 4.6   |
| 190                   | 0.25            | 0.080   | 4.5              | 4.1   |
| 300                   | 0.30            | 0.103   | 4.0              | 3.8   |

TABLE V. Data pertinent to the computation of  $K$  from Eq. (18) on the basis of a four-valley energy-band model.

| $T(^{\circ}\text{K})$ | $m_d^*$<br>(av) | $m_c^*$ | $K$<br>(calc.) | $m_t^*$ | $m_i^*$ |
|-----------------------|-----------------|---------|----------------|---------|---------|
| 77                    | 0.20            | 0.056   | 8.0            | 0.040   | 0.32    |
| 190                   | 0.25            | 0.080   | 4.8            | 0.059   | 0.28    |
| 300                   | 0.30            | 0.103   | 3.5            | 0.079   | 0.28    |

TABLE VI. Data used in Eq. (18) for the calculation of an "effective" number of equivalent ellipsoids for  $p$ -type PbTe.

| $T(^{\circ}\text{K})$ | $m_a^*$<br>(av) | $m_c^*$           | $K$ | $N_v$ |
|-----------------------|-----------------|-------------------|-----|-------|
| 77                    | 0.14            | 0.053             | 4.2 | 3.2   |
| 190                   | 0.19            | 0.080             | 4.5 | 2.7   |
| 300                   | 0.25            | 0.11 <sup>a</sup> | 4.7 | 2.5   |

<sup>a</sup> An extrapolated value.

complicates the analysis of the effective masses. The conductivity and density-of-states masses that are obtained from the analysis of the infrared data and of the reduced Fermi potential are average values associated with the entire valence band. They represent an average of the effective masses of all five valence-band maxima. Consequently, the simple relations used in the analysis of  $n$ -type material to obtain  $N_v$ ,  $m_i$ , and  $m_t$  are not expected to be applicable in the analysis of the valence band, because the zone-centered maximum cannot be treated as being exactly equivalent to those along the  $\langle 111 \rangle$  axes. However, it is instructive to apply these simple relations to the effective masses of the valence band on the assumption that all maxima are exactly alike. To this end we have calculated an  $N_v$  from Eq. (18) using values for  $K$  determined from magnetoresistance data,<sup>10</sup> namely 4.7 at 300°K and 4.2 at 77°K. The results of this calculation are presented in Table VI. The number of equivalent ellipsoids of constant energy in the valence band which is deduced from these values for the effective masses is seen to be something less than four. Although it is difficult to infer very much from this calculation, it does seem reasonable to conclude that the  $\langle 111 \rangle$  maxima are probably at the zone edge since the "effective" number deduced from Eq. (18) is even less than four. Such a conclusion is in line with the results reported in an investigation of the de Haas-van Alphen effect.<sup>22</sup> Moreover, these results are consistent with an interpretation that a zone-centered valence-band maximum is rather significant in the energy-band structure of the valence band. This conjecture is based on the idea that the number of ellipsoids would be four if the  $\langle 111 \rangle$  maxima dominated, could be as high as five if the  $\langle 000 \rangle$  and  $\langle 111 \rangle$  maxima had very similar characteristics, and would be less than four and approach unity as the  $\langle 000 \rangle$  maximum became the most prominent. In this regard, it should be pointed out that Allgaier has concluded from a careful analysis of the Hall effect that the zone-centered maximum does have an increasing importance as temperature increases.<sup>23</sup>

To further establish a correlation between the results presented here and those presented elsewhere in the literature for  $p$ -type material, we show in Fig. 3 the

results obtained by Dixon and Reidl.<sup>24</sup> The values presented here at 77 and 190°K are relatively close to theirs. However, there is actually less correlation than it appears because their values have been determined from the reflectivity minimum using the assumptions that  $\Omega^2 \gg 1$  and that  $k^2 \ll (n-1)^2$ . One would expect that these assumptions are reasonably well satisfied below 100°K, but above this temperature it becomes increasingly necessary to use the more exact relationship contained in Eq. (10). Perhaps one source of the discrepancy lies in the determination of the free-carrier density from the Hall coefficient. Because of the variation of the Hall coefficient with temperature arising from the zone-centered valence-band maximum, it becomes more difficult to determine the actual free-carrier concentration. (The Hall coefficient at 77°K was used in the analysis presented here.)

There remains one additional aspect of the infrared reflectivity that has not been evaluated. This has to do with the effects of the lattice polarization on the free-carrier dispersion. In the theoretical development for the utilization of the infrared-reflectivity minimum for calculating  $m_c$ , it was pointed out that a necessary condition is that the lattice polarization contributes a negligible amount to the reflectivity in the frequency range of the minimum.<sup>2</sup> By using Eq. (10) to obtain values for  $m_c$ , we have implicitly assumed that this is the case. (This same assumption is implicit in the infrared work of Dixon and Reidl.<sup>24</sup>)

The evaluation of the lattice contribution to the reflectivity is allied with the much broader problem of assessing the true polar character of the compounds in the PbS family. This is a piece of information which can be inferred by fitting the actual mobility with a theoretical mobility synthesized with the aid of the free-carrier effective masses presented here. Such a synthesis has been carried out in a companion article. It has been deduced from this synthesis that, for the free-carrier concentrations of the samples of this investigation, the lattice contributes less than 1% to the total reflectivity in the wavelength range of interest.

## CONCLUSIONS

In this investigation of  $3n$ - and  $2p$ -type single-crystalline samples of PbTe, we have determined the values of  $m_a$  and  $m_c$  as functions of temperature. The procedure for determining  $m_a$  utilized measurements of the thermoelectric power to establish  $\eta$  and of the Hall coefficient to establish  $N$ . We were thus able to obtain values for  $m_a$  between 77 and 300°K which agreed reasonably well with the values and temperature dependence reported in the literature. The procedure for determining  $m_c$  utilized measurements of  $\mu$  and the frequency of the reflectivity minimum in the infrared.

<sup>22</sup> P. Stiles, E. Burstein, and D. Langenberg, J. Appl. Phys. Suppl. 32, 2174 (1961).

<sup>23</sup> R. Allgaier, J. Appl. Phys. Suppl. 32, 2185 (1961).

<sup>24</sup> J. Dixon and H. Reidl, *Proceedings of the International Conference on the Physics of Semiconductors, Exeter 1962* (The Institute of Physics and the Physical Society, London, 1962), pp. 182-5.

This procedure also yielded values which agree generally with the literature. We found that the temperature dependences of both  $m_d$  and  $m_c$  are quite similar in samples having the same type of carrier. Such a result would be anticipated from the known values of the anisotropy ratio  $K$ . The fact that they did indeed have similar thermal characteristics may be considered as evidence of their correctness since they were obtained from very different procedures. The actual temperature dependence of the effective masses has been found to increase with increasing temperature and it approaches  $T^{0.5}$  for  $n$ -type and  $T^{0.8}$  for  $p$ -type material at 300°K. Furthermore, the values for  $m_c$  and  $m_d$  indicate that a four-valley model is to be preferred in the conduction band. In the valence band we infer that there is a zone-centered maximum, which increases in prominence with

increasing temperature, in addition to the other (probably four) valence-band maxima.

#### ACKNOWLEDGMENTS

I am especially indebted to Professor Arthur C. Smith of the Electrical Engineering Department of the Massachusetts Institute of Technology for his pertinent counsel throughout the course of this work. In addition, I am very grateful to Dr. Benjamin Lax of the National Magnet Laboratory in Cambridge, Massachusetts for extending to me the privilege of using the equipment of that laboratory, and to Dr. Dana Dickey and Michael Fulton of that Laboratory whose equipment and assistance made it possible to obtain the infrared reflectivity data. In addition, I wish to thank Dr. Robert E. Nelson for his assistance in the Hall measurement.

## Point Defect Studies in Gold by Electron Irradiation at Low Temperatures. I. Threshold Displacement Energy and Displacement Cross Section\*

WALTER BAUER AND A. SOSIN

*Atomics International, Division of North American Aviation, Inc., Canoga Park, California*

(Received 24 February 1964)

The damage production on 99.999% pure 0.00025-in.-thick gold foils was measured as a function of incident electron energy in the range from 1.3 to 2.2 MeV. The effective threshold displacement energy was measured to be near 35 eV. It was found that reasonable agreement between the experimental and theoretical values of the displacement cross section could only be achieved with an unusually low value of the resistivity of a Frenkel pair ( $\rho_F = 0.89 \times 10^{-4}$   $\Omega$ -cm/unit fractional concentration). By comparison, in copper the agreement between the theoretical and experimental cross section ( $\rho_F = 1.2 \times 10^{-4}$   $\Omega$ -cm/unit fractional concentration) is somewhat better. This is interpreted to indicate that directional effects in the displacement process are considerably more important in gold than in copper, and that, for energies near the threshold energy, displacements in gold are possible only in a small solid angle centered about one crystallographic direction, most likely the  $\langle 100 \rangle$  direction.

### I. INTRODUCTION

IN the study of point defects in metals, the noble metals—copper, silver, and gold—have received the major attention. Among these three, copper has been studied most intensively but gold has received increasing attention recently. The shift from copper to gold may be traced to the fact that, despite a large effort, the point defect characteristics in copper remain inadequately understood, and that the annealing characteristics in gold, following irradiation, are significantly different from copper and silver or, as a matter of fact, almost any metals which have been examined.

The threshold displacement energy in gold has been variously reported to be  $>40$  eV,<sup>1</sup> near 40 eV,<sup>2</sup> and be-

tween 33 and 36 eV.<sup>3</sup> The experiments discussed in this paper were undertaken to measure the damage production as a function of the electron energy and thus to afford a comparison between the experimental and theoretical values of the displacement cross section.

In part II of this paper a description of the experimental equipment and techniques is given. Part III deals with the experimental results. The theoretical displacement cross section and a comparison of experimental and theoretical results is given in part IV. A discussion of the results is given in part V.

### II. EXPERIMENTAL METHODS

#### A. Specimen Preparation

In order to achieve minimum energy degradation of the bombarding electrons in the specimens 0.00025-in.-

\* This work was supported by the U. S. Atomic Energy Commission.

<sup>1</sup> P. G. Lucasson and R. M. Walker, *Phys. Rev.* **127**, 485 (1962).

<sup>2</sup> R. B. Minnix and P. E. Shearin, *Bull. Am. Phys. Soc.* **8**, 196 (1963).

<sup>3</sup> W. Bauer and A. Sosin, *J. Appl. Phys.* **35**, 703 (1964).